Acid−Base Properties of Fulleropyrrolidines: Experimental and Theoretical Investigations

Francis D'Souza,*,† Melvin E. Zandler,† Gollapalli R. Deviprasad,† and Wlodzimierz Kutner‡

Department of Chemistry, Wichita State University, Wichita, Kansas 67260-0051, and Institute of Physical Chemistry, Polish Academy of Sciences, Kasprzaka 44/52, 01-224 Warsaw, Poland

Received: March 22, 2000; In Final Form: May 11, 2000

The acid−base equilibria of 2-(*n*-alkyl)fulleropyrrolidines and *N*-methyl-2-(*n*-alkyl)fulleropyrrolidines in aqueous micellar media of a sodium dodecyl sulfate surfactant are examined experimentally and modeled theoretically by using ab initio 3-21G(*) methods. The pK_a values, for 2-(*n*-alkyl)fulleropyrrolidines and *N*-methyl-2-(*n*-alkyl)fulleropyrrolidines, determined both by HCl and NaOH titration with potentiometric detection of the end point, are equal to 6.3 ± 0.1 and 7.5 ± 0.1, respectively, and are independent of the alkyl chain length within a range of C1 to C8. The obtained results indicate that the fullerene cage fused to a pyrrolidine ring increases the acidity of the protonated pyrrolidine nitrogen mainly due to the induced electronic effects and, to a smaller extent, by structural effects. The 3-21G(*) estimated free energy difference, ΔE (with solvation corrections incorporated based on the Cramer-Truhlar SM5.4 solvation model), between the protonated and unprotonated fulleropyrrolidines, and the experimental pK_a values have been correlated for 37 different nitrogenous bases. A $0 <$ pK_a <14 range was covered with these bases which include the presently investigated fulleropyrrolidines. Correlation between the calculated ΔE and experimental pK_a values is good ($\Delta E = 2.3126$ p$K_a + 280.49$, correlation coefficient is equal to 0.95) and indicates that the effect on pK_a of the micellar environment, utilized in the present study for solubilization of the fulleropyrrolidines, is negligible. Comparison of the calculated HOMO and LUMO energy levels for the protonated and free-base forms of the investigated fulleropyrrolidines indicates that electron deficiency of the C_{60} cage and the HOMO−LUMO energy gap caused by *N*-protonation are increased. This result agrees well with the earlier electrochemical results for fulleropyrrolidinium cations.

Introduction

Physicochemical characterization of functionalized fullerenes is an area of growing interest.[1] Studies performed so far have revealed properties that make functionalized fullerenes useful for such diverse areas as biomedical applications and designing molecular electronic devices as well as for constructing solar energy harvesting systems.[1−3] Fulleropyrrolidine (Scheme 1), an organofullerene derivative in which a pyrrolidine ring is fused to a 6,6 ring junction of the C_{60} cage, is one of the widely studied fullerene derivatives.[4] One of the interesting properties of fulleropyrrolidines is their acid−base property. The acid−base equilibria provide ways to determine equivalent weights, percent composition, and solution concentrations. Moreover, structure−reactivity aspects, i.e., the effect of the fullerene cage on the pyrrolidine nitrogen reactivity, can also be probed. The latter property is highly useful for further appending another redox active group or chromophore to form fullerene-bearing dyad addends. In this respect, several dyads appended through the pyrrolidine nitrogen are investigated.[2,5−6]

It is reported that in dioxane:water, 85:15 (v:v), the pK_a value for 2-substituted *N*-methylfulleropyrrolidine (substituent = CH_2-$OCH_2CH_2OCH_2CH_2OCH_3$) is equal to 5.6.[4] This value is considerably lower than the corresponding *N*-methylpyrrolidine (pK_a = 11.1).[4] Studies of conjugated acid−base and redox equilibria of genuine C_{60} revealed a weak basic nature of both its mono- and dianion.[7−9] In the present study, we report on the acid−base equilibria for two types of fulleropyrrolidine derivatives, i.e., fulleropyrrolidines bearing a secondary or tertiary nitrogen atom in their free-base forms (Scheme 1) in aqueous micellar media of a sodium dodecyl sulfate (SDS) surfactant. For the acid−base equilibria study, the presently employed micellar microheterogeneous aqueous system is advantageous over a mixed organic solvent system because of less complex composition and higher dielectric permittivity.[10] Moreover, the polar pyrrolidine group is expected to be located close to or in the aqueous phase, both in its free-base and protonated form, while the fullerene cage is incorporated into a hydrophobic part of the micelle for the investigated fulleropyrrolidines. Hence, the values of the experimentally determined proton dissociation constants are expected to be close to those anticipated for aqueous systems. That is, the effect of the micellar medium on the pK_a values should be small.

SCHEME 1

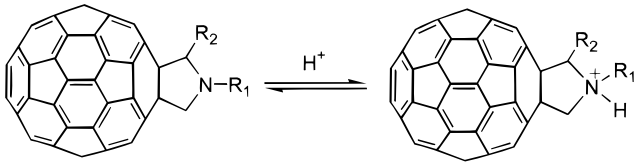

R_1 = H or CH_3; R_2 = C_4H_9, C_8H_{17}, $C_{12}H_{25}$

To get further insight into the studied acid−base properties, the protonation equilibria and electronic structures of the fulleropyrrolidines are modeled here by using ab initio 3-21G(*) calculations. These calculations take into account the solvent

* Author to whom correspondence should be addressed.
† Wichita State University.
‡ Polish Academy of Sciences.

10.1021/jp001081o CCC: $19.00
Published on Web 07/01/2000

correction factors based on the method of Cramer and Truhlar.[11] For primary, secondary, tertiary, and aromatic nitrogenous bases, the calculated free energy difference between protonated and unprotonated nitrogenous bases is correlated with the experimentally determined pK_a values available in the literature. The effect of protonation on energy values of the highest occupied molecular orbitals (HOMOs) and the lowest unoccupied molecular orbitals (LUMOs) of fulleropyrrolidines is also investigated.

Experimental Section

The synthesis and purification of fulleropyrrolidines is described elsewhere.[12,13] The fulleropyrrolidinium trifluoroacetate was prepared by reacting fulleropyrrolidine and trifluoroacetic acid. The structures of the synthesized compounds were established on the basis of elemental analysis as well as on the FAB mass, NMR, and UV−visible absorption spectroscopy results. Potentiometric pH titrations were performed with the use of a Metler MP 230 digital pH-meter and a glass combination electrode. The concentration of SDS (Aldrich) utilized for preparation of aqueous micellar systems of the fulleropyrrolidines was kept above the critical micellar concentration (CMC) value.[10] Stock CS_2 solutions of fulleropyrrolidines were prepared from weighing portions. The fulleropyrrolidines were solubilized in aqueous micellar systems by simultaneous sonication and nitrogen gas purging through a two-phase system comprising the CS_2 stock solution of fulleropyrrolidine and SDS aqueous system. Doubly distilled decarbonated water was used for preparation of the solutions. The UV−visible absorption spectra were recorded on a Shimadzu model 1600 spectrophotometer. All measurements were performed at 25 ± 1 °C.

The computational calculations were performed at the ab initio 3-21G(*) level with the SPARTAN PRO[14] and GAUSSIAN 98[15] software packages on various PCs and a SGI ORIGIN 2000 computer. The aqueous solvation correction factors used were based on class IV atomic charges and the first solvation shell model of Cramer and Truhlar[11] incorporated in the SPARTAN PRO software package. Different 37 nitrogenous bases of pK_a values ranging from 0 to 14 were modeled by using this computational approach, and the results are compared with the presently studied fulleropyrrolidines.

Results and Discussion

Solubilization of Fulleropyrrolidines in Aqueous SDS Micellar Systems. Compartmentalization of fullerenes and their derivatives in microheterogeneous media is widely recognized as an efficient way of solubilizing these compounds in aqueous systems for chemical and biological studies. Triton X-100, a neutral surfactant, is often utilized for that purpose.[16−18] Sodium dodecyl sulfate, an anionic surfactant used in the present study, is found here to work equally well for solubilizing fulleropyrrolidines.

Figure 1 shows the UV−visible absorption spectra of 2-(*n*-butyl)fulleropyrrolidine both in its free-base, i.e., neutral, and protonated forms. The neutral form exhibits absorption bands at 266, 280, and 360 nm(sh) (Curve *1* in Figure 1) similar to those reported for *N*-methylfulleropyrrolidine in Triton X-100.[18] The intensity ratio of the absorption peaks varies slightly with the change of the fulleropyrrolidine concentration, presumably, due to the presence of different forms of aggregated species in solution. Interestingly, the protonated form, prepared by lowering the solution pH, exhibits blue-shifted bands located at 262, 320, and 360 nm(sh) (Curve *2* in Figure 1). For the protonated form, the UV band at 262 nm is increased considerably as

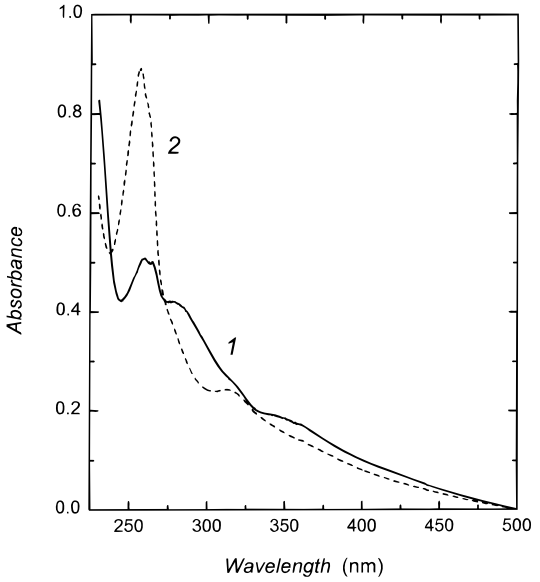

Figure 1. UV−visible absorption spectra for ∼10^{-2} mol dm^{-3} sodium dodecyl sulfate micelles of 2-(*n*-butyl)fulleropyrrolidine (curve *1*) and 2-(*n*-butyl)fulleropyrrolidinium chloride (pH 3.25) (curve *2*).

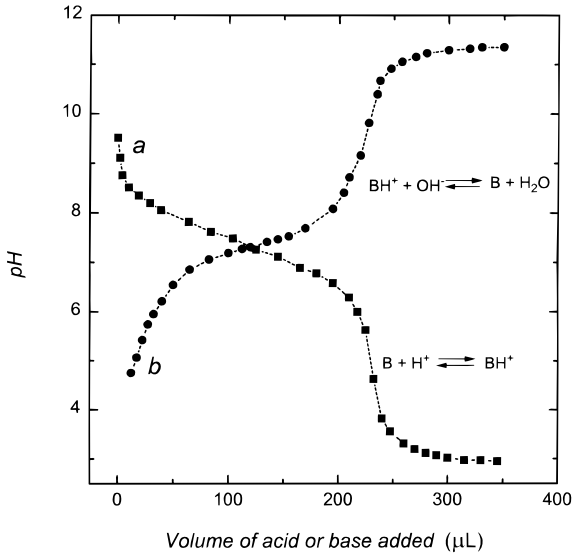

Figure 2. Titration curves for ∼10^{-2} mol dm^{-3} sodium dodecyl sulfate micelles of ∼3 mmol dm^{-3} 2-(*n*-alkyl)fulleropyrrolidine) and HCl (curve *a*) and ∼3 mmol dm^{-3} 2-(*n*-alkyl)fulleropyrrolidinium trifluoroacetate and NaOH (curve *b*).

compared to that for the unprotonated one which could be due either to interaction of the positive charge on the nitrogen atom of the pyrrolidine ring with the fullerene cage or to disintegration of the aggregates, or different extents of solvation, or combination of these effects.

Determination of the pK_a Values for Fulleropyrrolidines. The pK_a values for fulleropyrrolidines were determined both by HCl titration of fulleropyrrolidines and NaOH titration of the conjugated fulleropyrrolidinium cations. For a given fulleropyrrolidine derivative, the pK_a values, calculated from the derivative modes of the Henderson−Hasselbalch plots for both acid and base titration curves, were equal within the experimental error. Figure 2 shows representative acid−base titration curves for the *N*-methyl-2-(*n*-alkyl)fulleropyrrolidine derivative. The determined pK_a values are equal to 6.3 ± 0.1 and 7.5 ± 0.1 for 2-(*n*-alkyl)fulleropyrrolidines and *N*-methyl-2-(*n*-alkyl)-fulleropyrrolidines, respectively. These values are independent of the chain length of the 2-(*n*-alkyl) group attached to the

SCHEME 2

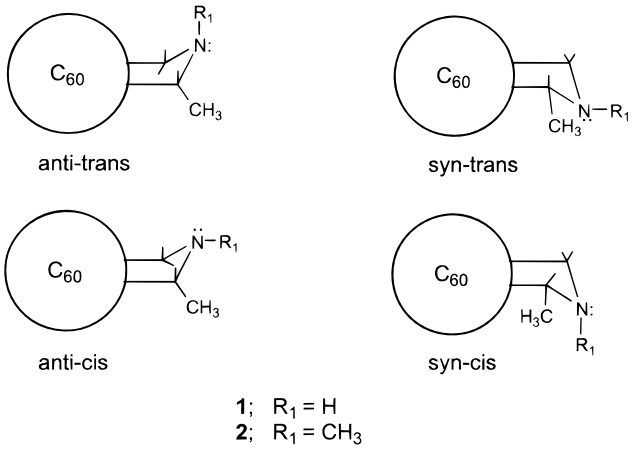

1; $R_1 = H$
2; $R_1 = CH_3$

pyrrolidine ring within a range of C1 to C8. Also, variation of the SDS concentration from 1.1×10^{-2} to 4.33×10^{-2} mol dm^{-3} revealed no appreciable changes in the determined pK_a values. On one hand the pK_a values for fulleropyrrolidines are 3 to 4 units smaller than those for the pyrrolidine derivatives and, on the other, the pK_a values determined in the present study are 1 to 2 units larger than those reported earlier for dioxane:water, 85:15 (v:v), solutions.[4] The latter difference could be due either to increased preferential solubilization of the neutral fulleropyrrolidine in the nonaqueous solution[19] or to the effects of different substituents.

The micellar media utilized here for solubilization of fulleropyrrolidines appeared to be highly advantageous for acid−base titration since the dodecyl sulfate micelles, with a size varying from 2 to 4 nm, can easily accommodate one or more fulleropyrrolidine moieties.[10] The estimated dipole moment values for fulleropyrrolidine and fulleropyrrolidinium cations were fairly high (vide infra). These high values suggest that the polar pyrrolidine parts of the molecules, both in their acidic and free-base forms, are located close to water molecules of the aqueous phase. To verify the effect of micellar media on the determined pK_a values, control acid−base titrations were performed for imidazole and morpholine in dodecyl sulfate micelles. The determined pK_a values are found to be 6.86 and 8.41 for imidazole and morpholine, respectively, which compare with reported values of 6.99 and 8.49 in aqueous solutions.[23]

Modeling Studies. The structure−activity aspects of the protonation equilibrium and the electronic structure of fulleropyrrolidines are modeled by using ab initio calculations at the 321-G(*) level. For a given fulleropyrrolidine derivative, at least four stable conformers are conceivable (Scheme 2), depending upon pyrrolidine ring puckering and disposition of the substituent at the nitrogen and 2,2′-carbon atoms. The lowest energy (fully optimized to a stationary point on the Born−Oppenheimer potential energy surface) conformer of *N*-methyl-2-methylfulleropyrrolidine, **2**, is found to be the one similar to that reported recently in a crystal structure.[20] In this conformer, the pyrrolidine ring is puckered in such a way that the 2-methyl group is syn to the nitrogen atom and the N−CH_3 group is trans to the 2-methyl group. A similar low energy conformer was obtained for *N*-methyl-2-methylfulleropyrrolidinium cation, **2**+$\mathbf{H}^+$. By the same procedure, the lowest energy conformer for 2-methylfulleropyrrolidine, **1**, is found to be syn-cis while that for 2-methylfulleropyrrolidinium cation, **1**+$\mathbf{H}^+$ is syn (see Table 4).

To estimate the pK_a of the nitrogenous bases by ab initio methods, the following protonation equilibrium was considered:

$$BH^+_{solv} \leftrightarrows B_{solv} + H^+_{solv} \quad (1)$$

The thermodynamic constant for this equilibrium is given as

$$K_a = [B][H^+]/[BH^+] = \exp(-\Delta G°/RT) = 10^{-pKa} \quad (2)$$

To avoid explicit consideration of the H^+_{solv} structural energy at the 3-21G(*) level, the energy change for equilibrium (eq 3) was calculated by examining the half reactions (eqs 4 and 5).

$$BH^+_{solv} + H_2O_{solv} \leftrightarrows B_{solv} + H_3O^+_{solv} \quad (3)$$

$$BH^+_{solv} \rightarrow B_{solv} \quad (4)$$

$$H_3O^+_{solv} \rightarrow H_2O_{solv} \quad (5)$$

The free energy change for equilibrium (eq 3) can be represented as the difference between the free energy change for the half reactions (eqs 4 and 5). The free energy change for half reaction 5 was determined as the intercept of the least-squares fit of 37 nitrogenous bases, B (vide infra). The free energy change for equilibrium (eq 4) was computed according to Scheme 3, where the solvation energy values were calculated on the basis of class IV atomic charges and the first solvation shell model SM5.4 of Cramer and Truhlar[11] by using the SPARTAN−PRO software.[14]

SCHEME 3

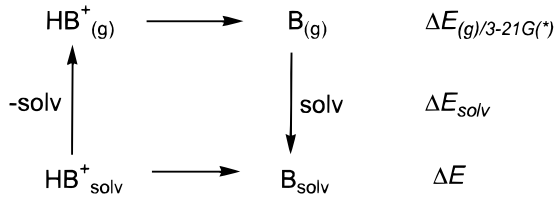

$$\Delta G = \Delta G_{(g)} + \Delta G_{solv} \simeq \Delta E_{(g)/3\text{-}21G(*)} + \Delta E_{solv} = \Delta E \quad (6)$$

In the above scheme, the differences in energy, ΔE, have been approximated to the differences in the free energy changes by neglecting the entropy term, $\Delta S_{(g)}$.[21] No effort was undertaken here to compute $\Delta S_{(g)}$ explicitly (sample lengthy computations of zero-point energy, temperature, and entropy corrections from vibrational frequencies showed little improvement in least-squares fit), although entropy terms are presumably present in ΔE_{solv}.[22] The values of heat of protonation[21] and the aqueous solvation correction factors, calculated for each conformer, are listed in Table 1.

From Table 1 it follows that the calculated ΔE values for the low energy conformers of **1** and **2** are comparable and, for the different isomers of a given fulleropyrrolidine, these values vary within ±1.5 kcal/mol. To be confident in the computed values, we verified the adopted approach by correlating the computed ΔE values with the literature pK_a values for 37 different nitrogenous bases, including primary, secondary, tertiary, and aromatic nitrogenous bases. Thus, a range of $0 <$ pK_a < 14 was covered. Table 2 lists the experimental pK_a values along with the computed ΔE values, while Figure 3 shows a plot of ΔE versus pK_a for the different bases investigated in the present study. Very small molecules, like NH_3 and hydrazine, are not included in the plot due to probable large error of the solvation energy calculations.[11] From the slope and intercept of the straight-line plot, the following equation is derived for computing the pK_a values according to the present model:

TABLE 1: Ab Initio 3-21G(*) Calculated Gas-Phase and Solvation-Corrected Deprotonation Energies (eq 4) for the Different Geometric Isomers of Fulleropyrrolidine Derivatives

compound	isomer	$\Delta E_{(g)/3-21G(*)}$[b], kcal/mol	ΔE_{solv}, kcal/mol	ΔE, kcal/mol
1	anti-trans	240.465	56.665	297.130
	syn-cis[a]	240.645	56.309	296.954
	anti-cis	241.410	56.877	298.287
	syn-trans	241.433	57.007	298.440
2	anti-trans	244.850	52.320	297.170
	syn-cis	245.085	51.334	296.419
	anti-cis	244.060	51.680	295.740
	syn-trans[a]	245.310	51.222	296.532

[a] Lowest energy isomer. [b] Since no zero point or temperature corrections were made, the absolute gas-phase deprotonation values reported here are expected to be high.

TABLE 2: Ab Initio 3-21G(*) Calculated Energy Differences, ΔE, and pK_a Values of the Investigated Series of Nitrogen Bases after Incorporation of Solvent Correction Factors

	compound	$(pK_a)_{exp}$[a]	ΔE, kcal/mol[b]	$(pK_a)_{cal}$[c]
1	*N,N,N*-trimethylguanidine	13.90	316.827	15.71
2	amidinomethane	12.40	313.551	14.30
3	benzamidine	11.60	310.604	13.02
4	pyrrolidine	11.31	306.387	11.20
5	piperidine	11.12	304.754	10.49
6	2-methyl piperidine	10.95	304.718	10.48
7	dimethylamine	10.77	303.253	9.84
8	cyclohexylamine	10.64	307.116	11.51
9	ethylamine	10.63	306.641	11.31
10	methylamine	10.62	306.104	11.08
11	*N*-methyl-2-methylpiperidine	10.22	303.479	9.94
12	*N*-methyl-2-methylpyrrolidine	10.20	303.147	9.80
13	*N*-methylpiperidine	10.19	302.839	9.66
14	*N*-methyl-3-pyrroline	9.88	299.460	8.20
15	trimethylamine	9.80	300.989	8.86
16	morpholine	8.49	299.049	8.02
17	aziridine	8.04	298.922	7.97
18	2-methyl-2-pyrroline	7.87	296.423	6.89
19	2-methylimidazole	7.86	297.961	7.55
20	4-methylimidazole	7.55	297.213	7.23
21	*N*-methyl-2-alkylfulleropyrrolidine[d]	7.50	296.529	6.94
22	*N*-methylimidazole	7.06	297.176	7.22
23	imidazole	6.99	295.542	6.51
24	2-alkylfulleropyrrolidine[e]	6.30	296.951	7.12
25	hydroxylamine	6.03	292.628	5.25
26	2,2,2-trifluoroethylamine	5.70	291.960	4.96
27	pyridine	5.17	291.361	4.70
28	aniline	4.60	290.184	4.19
29	4-chloroaniline	3.99	287.180	2.89
30	5-methylpyrazole	3.32	290.162	4.18
31	1,5-dimethylpyrazole	2.89	289.508	3.90
32	pyrazole	2.61	288.203	3.34
33	pyridazine	2.33	286.927	2.78
34	1-methylpyrazole	2.09	287.696	3.12
35	pyrimidine	1.30	285.944	2.36
36	4-nitroaniline	1.01	280.489	0.00
37	pyrazine	0.60	283.002	1.09
38	water	0.00	287.110	

[a] pK_a values of the nitrogenous bases are taken from ref 23. [b] Solvation-corrected protonation energies (eq 4). [c] See text for details. [d] Calculated values are for the syn-trans isomer of **2**. [e] Calculated values are for the syn-cis isomer of **1**.

$$pK_a = (280.49 - E_{3-21G(*)(sol)})/2.3126 \qquad (7)$$

The computed pK_a values agree with the experimental values within a standard deviation of 0.87 (Table 2). Earlier, similar plots involving experimental pK_a and experimental heats of neutralization,[24] as well as experimental free energy change and calculated free energy change,[25] have been compared for these purposes. A linear dependence with correlation coefficient equal to 0.95 is obtained in Figure 3, indicating a good agreement between the free energy difference calculated using the adopted method and the experimental pK_a values. The intercept of the plot, which is equal to the energy change for half reaction 5, is found to be 280.3 kcal/mol and compares with the explicitly calculated value of 287.1 kcal at the 3-21G(*) level (where H_3O^+ optimizes to a planar geometry!). The pK_a values of fulleropyrrolidines, determined experimentally in the present study, match well to the plot, suggesting that the aqueous micellar media used here do not alter the experimental pK_a values significantly from that expected for aqueous solutions with no micelles.

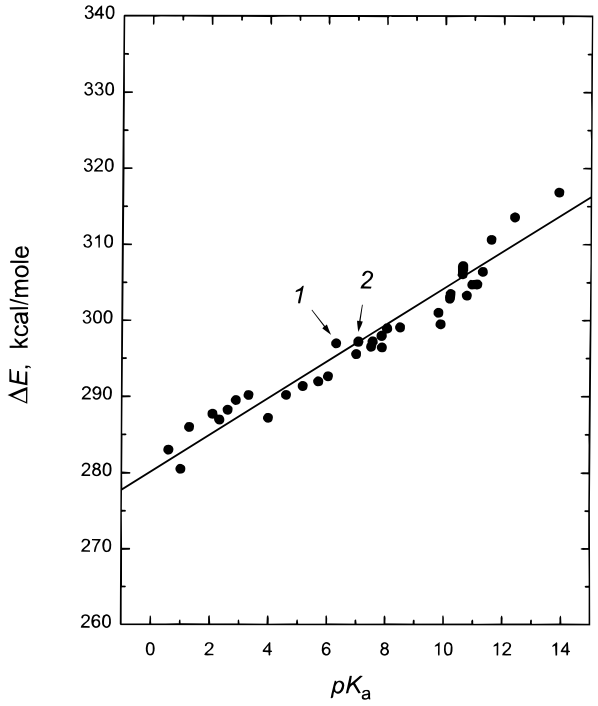

Figure 3. Plot of the 3-21G(*) calculated energy difference, ΔE, between the protonated and unprotonated nitrogenous bases, corrected for solvation, as a function of the experimental values. The datum point for 2-(*n*-alkyl)fulleropyrrolidine, **1**, and the datum point for *N*-methyl-2-(*n*-alkyl)fulleropyrrolidine, **2**, are indicated with arrows.

The remarkably good correlation between the calculated ΔE values and experimental pK_a values is commendable. Furthermore, the correlation approach used here is much better suited to large molecular systems, such as fulleropyrrolidines, than a higher level computational model based on first principles. Preliminary 6-31G* calculations performed on the same series of compounds indicate that the resulting data fit is not better than that for the 3-21G(*) calculations and correlated methods do not seem to be necessary for good results.

Further modeling studies have been performed to quantitate the factors responsible for lowering the pK_a values of fulleropyrrolidines. Two factors—namely, (i) electronic, which include the inductive and conjugative effects caused by the fused fullerene moiety, and (ii) structural, which include the different geometrical isomers (Scheme 2) and different degrees of nonplanarity of pyrrolidine ring—are considered. Since the different geometrical isomers of either **1** or **2** have a small effect on ΔE (Table 1), no further discussions are offered on this particular issue here. Scheme 4 shows the studied model molecules used to evaluate these factors. Compound **3**, i.e., 2-methylpyrrolidine in its lowest energy syn-cis form, is considered as a standard for 2-(*n*-alkyl)-substituted pyrrolidine. Compound **4**, in which the syn-cis isomer of 2-methylpyrrolidine

SCHEME 4

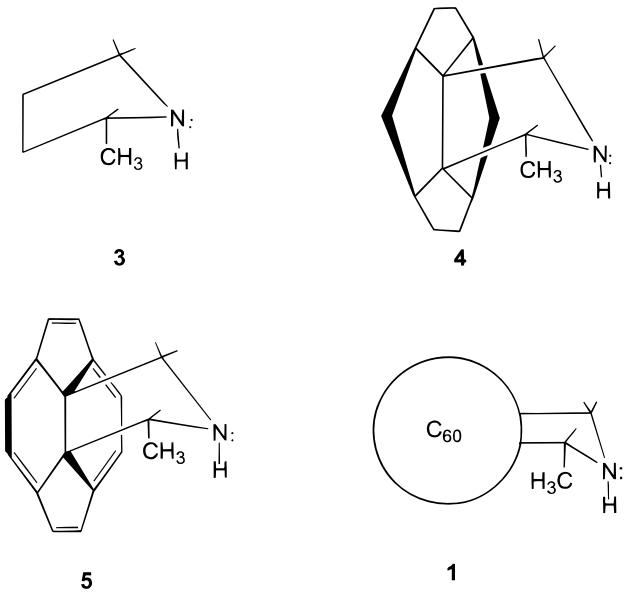

TABLE 3: Ab Initio 3-21G(*) Calculated Energies for the Protonated and Free-Base 3,4-Substituted Pyrrolidines in the Syn-Cis and Planar-Cis Conformations

compound[a]	configuration	$E_{BH^+(g)}$, Hartrees	$E_{B(g)}$, Hartrees	ΔE, kcal/mol[b]
3	syn-cis	−249.199449	−248.797405	−305.327
	planar-cis	−249.191143	−248.791372	−304.296
	$(\Delta E)_{stru}$, kcal/mol	5.21	3.79	
4	syn-cis	−632.771100	−632.360357	−305.316
	planar-cis	−632.761763	−632.352528	−304.645
	$(\Delta E)_{stru}$, kcal/mol	5.86	4.91	
5	syn-cis	−703.291727	−702.884597	−298.657
	planar-cis	−703.277408	-−702.871354	−299.000
	$(\Delta E)_{stru}$, kcal/mol	8.99	8.31	
1	syn-cis	−2430.625564	−2430.242049	−296.968
	planar-cis	−2430.612644	−2430.229571	−298.035
	$(\Delta E)_{stru}$, kcal/mol	8.11	7.83	

[a] See Scheme 4 for the structural formulae. [b] Solvated deprotonation energy values (eq 6).

ring is fused to a dicyclopentapentalene macrocycle mimics the partial C_{60}-like surface with all saturated bonds. Compound **5**, with pyrrolidine ring fused to a cyclopentaacenaphthylene ring, mimics a C_{60} part with unsaturated double bonds. Finally, the syn-cis isomer of **1** is also considered. The energy values for these molecules, calculated as described in the preceding paragraphs in their syn-cis and planar-cis conformations, are listed in Table 3. The planar-cis conformers were obtained by constraining the five pyrrolidine ring atoms to lie in a plane.

Examination of Table 3 reveals the following energetic and molecular features. The difference in ΔE between syn-cis **3** and syn-cis **4** is 0.01 kcal/mol, indicating that the substitution of a saturated macrocycle at the 3,4 positions of the pyrrolidine ring would not influence the acidity of ring nitrogen significantly, although changing the distortion and rigidity of the pyrrolidine ring might cause a change in ΔE. The ΔE value drops by 6.67 kcal/mol going from syn-cis **3** to syn-cis **5** which corresponds to a pK_a decrease by 2.88 units, as estimated by extrapolation of the linear plot in Figure 3. The difference in ΔE between syn-cis **3** and syn-cis **1** is 8.36 kcal/mol and corresponds to a drop in pK_a by 3.61 units. These results indicate that the electronic effects caused by the unsaturated bonds of cyclopentaacenaphthylene and C_{60} lower the pK_a value of pyrrolidine, and this effect increases with increasing the number of unsaturated bonds. This electronic effect could be either an inductive effect or a conjugative effect or a combination of both. However, the conjugative effects do not appear to be significant, as discussed below in this section.

The energy required to convert the syn-cis conformer to a planar-cis conformer, $(\Delta E)_{stru}$, both for the protonated, BH^+, and free-base, B, forms of pyrrolidines (Table 3), indicate that the protonated pyrrolidine rings are more difficult to be made planar than the free-base rings, and, the pyrrolidine ring fused to unsaturated cyclopentaacenaphthylene or C_{60} moieties needs additional 3−4 kcal/mol of energy to make the ring planar. The resulting effect of this structural change on ΔE is, however, minor. That is, the difference in ΔE between the syn-cis and planar-cis conformer of a given compound is ∼1 kcal/mol, which corresponds to a pK_a change of less than 0.5. This magnitude of ΔE is almost similar to that observed for different geometrial isomers (Table 1). Interestingly, this effect is opposite for compounds **1** and **5**, as compared to those for compounds **3** and **4**. That is, the planar-cis isomers of compounds **1** and **5** are more basic than the syn-cis isomers. In summary, the induced electronic effect caused by the fused fullerene ring is a major factor responsible for lowering the pK_a values of fulleropyrrolidines, and the structural effects contribute to a lesser extent.

Several physical properties of C_{60} and different conformers of fulleropyrrolidine derivatives, computed by using the 3-21G(*) method, are summarized in Table 4. For the protonated derivatives, the calculated solvation energy values appeared to be by an order of magnitude higher than those for the corresponding free-base fulleropyrrolidines. The gas-phase dipole moment values vary between 2.69 and 4.69 D for unprotonated fulleropyrrolidines, while these values range between 19.02 and 20.30 D for protonated derivatives. Axes of these dipoles pass through the pyrrolidine nitrogen atoms. The dipole moment calculations support our initial hypothesis that the polar pyrrolidine nitrogen is located near water molecules of the aqueous phase of the micellar microheterogeneous media. The total Mülliken charge on the pyrrolidine nitrogen atom given in Table 4, representing its basicity, decreases because of protonation.

Comparison of the HOMO−LUMO energy levels with the frontier molecular orbitals of the investigated fulleropyrrolidines leads to the following conclusions. Triple degeneracy of LUMO and 5-fold degeneracy of HOMO of C_{60}[26] are split in the case of fulleropyrrolidines as a result of lowering symmetry and lifting of the two fullerene carbon atoms connected to the pyrrolidine ring by about 0.3 Å above the C_{60} pseudo sphere. Inspection of the LUMO energy levels for the derivatives in a gas phase (Table 4) indicates that the electron deficiencies of the fulleropyrrolidinium cations are increased as compared to those for the unprotonated derivatives. Earlier, such LUMO energy levels, obtained by semiempirical calculations, have been utilized to compare the redox properties of fullerene derivatives.[27,28] The HOMO energy levels also indicate this trend, suggesting that ionization of the protonated fulleropyrrolidines would be difficult. The HOMO−LUMO energy gap for fulleropyrrolidines appear to be by nearly 0.35 eV smaller than that for C_{60}, and is by 0.1 to 0.15 eV smaller than that for the protonated fulleropyrrolidines. This predicted increased electron deficiency of fulleropyrrolidinium cations is consistent with the easier electrochemical reduction of fulleropyrrolidinium cations than fulleropyrrolidines, as reported earlier by others[29] and us.[12,13]

The frontier molecular orbital representations shown in Figure 4 for the HOMO and LUMO of the free-base and protonated syn-trans isomer of **2** indicate that the HOMO of **2** involves

TABLE 4: Ab Initio 3-21G(*) Calculated Physical Properties of C_{60} and Fulleropyrrolidine Derivatives

compd	conformer[a]	$E_{3-21G(*)}$, Hartrees	rel. E^b	ΔE_{sol}, kcal/mol	μ, D	charge on N atom	LUMO-2, eV	LUMO-1, eV	LUMO, eV	HOMO, eV	HOMO+1, eV	Δ(HOMO−LUMO), eV
C_{60}		−2259.047589		−4.496	0.00		−0.629	−0.629	−0.629	−8.330	−8.330	7.701
1	anti-trans	−2430.240278	1.11	−8.120	2.69	−0.678	−0.011	−0.309	−0.525	−7.889	−8.072	7.364
	syn-cis	**−2430.242049**	**0.00**	**−8.293**	**2.69**	**−0.684**	**−0.012**	**−0.311**	**−0.524**	**−7.889**	**−8.073**	**7.365**
	anti-cis	−2430.238772	2.06	−7.908	4.60	−0.715	0.054	−0.241	−0.458	−7.810	−8.005	7.352
	syn-trans	−2430.240793	0.79	−7.595	4.59	−0.715	0.052	−0.242	−0.457	−7.811	−8.005	7.354
1-H$^+$	anti	−2430.623483	1.31	−64.785	19.52	−0.784	−2.400	−2.784	−2.937	−10.435	−10.508	7.497
	syn	**−2430.625564**	**0.00**	**−64.602**	**19.50**	**−0.789**	**−2.406**	**−2.790**	**−2.938**	**−10.436**	**−10.509**	**7.498**
2	anti-trans	−2469.051069	2.90	−5.328	3.34	−0.671	0.014	−0.281	−0.502	−7.854	−8.047	7.352
	syn-cis	−2469.051131	2.86	−6.880	3.37	−0.678	0.015	−0.283	−0.499	−7.852	−8.042	7.354
	anti-cis	−2469.053551	1.47	−4.716	4.69	−0.698	0.063	−0.232	−0.450	−7.799	−7.995	7.349
	syn-trans	**−2469.055688**	**0.00**	**−5.144**	**4.56**	**−0.681**	**0.053**	**−0.243**	**−0.458**	**−7.810**	**−8.006**	**7.352**
2-H$^+$	anti-trans	−2469.441263	3.36	−57.648	19.79	−0.763	−2.351	−2.728	−2.897	−10.378	−10.458	7.481
	syn-cis	−2469.441699	3.08	−58.214	19.86	−0.770	−2.357	−2.739	−2.899	−10.382	−10.461	7.502
	anti-cis	−2469.442286	2.72	−56.396	20.23	−0.772	−2.339	−2.719	−2.880	−10.371	−10.450	7.491
	syn-trans	**−2469.446615**	**0.00**	**−56.366**	**20.30**	**−0.774**	**−2.340**	**−2.723**	**−2.877**	**−10.368**	**−10.447**	**7.492**

[a] See Scheme 2 for details. [b] With respect to the lowest energy isomer (indicated in bold) of the corresponding fulleropyrrolidine derivative.

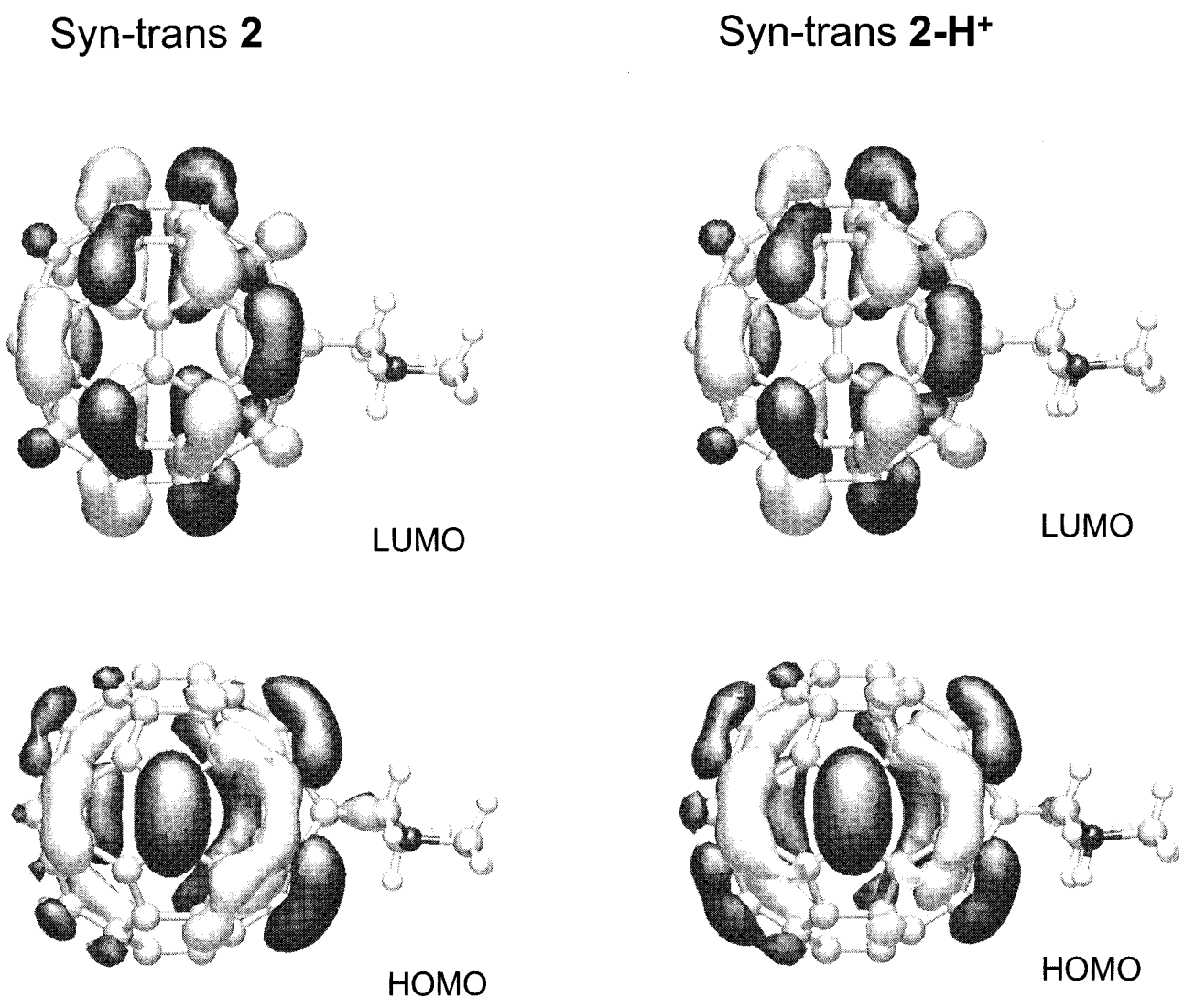

Figure 4. Frontier HOMO and LUMO for the syn-trans isomer of *N*-methyl-2-(*n*-alkyl)fulleropyrrolidine, **2**, and *N*-methyl-2-(*n*-alkyl)-fulleropyrrolidinium cation, **2**+**H**$^+$, calculated at the 3-21G(*) basis set keeping the contour level of 0.002 e au^{-3}. The darker and lighter shades represent positive and negative coefficients, respectively.

pyrrolidine ring carbon atoms to a very small extent in addition to the fullerene cage carbon atoms. However, the LUMO of **2** and HOMO and LUMO of **2**+**H**$^+$ involve virtually no pyrrolidine ring nitrogen or carbon atoms but are primarily localized on the fullerene carbon atoms. As expected, the nodal sequence for **2** and **2**+**H**$^+$ remains more or less the same. The lack of considerable contribution of orbital coefficients extending to the pyrrolidine ring suggests the absence of conjugative effects on the pyrrolidine ring atoms due to the fused C_{60} moiety.

In summary, the present investigations indicate that the acidity

of the nitrogen atom of the pyrrolidine ring fused to the fullerene cage is increased as compared to that of unsubstituted pyrrolidine, primarily due to the inductive electronic effects and, to a lesser extent, the structural effects. The experimental results agree well with the trends predicted by ab initio calculations at the 3-21G(*) level. Also, our studies indicate that quaternalization of the pyrrolidine nitrogen increases both the electron deficiency of the C_{60} cage and the HOMO−LUMO energy gap, a result that readily agrees with the earlier electrochemical investigations performed on fulleropyrrolidinium cations.[12,13,29]

Acknowledgment. Financial support of the U.S.−Polish M. Sklodowska-Curie Fund II (PAN/NSF-96-275, to F.D. and W.K.) and of the Dreyfus Foundation (to M.E.Z.), as well as that of the donors of the Petroleum Research Fund, administered by the American Chemical Society (to F.D.), is gratefully acknowledged. Also, the authors are thankful to the High Performance Computing Center of the Wichita State University for lending SGI ORIGIN 2000 computer time.

References and Notes

(1) See, for example: *Fullerenes*: *Recent Advances in the Chemistry and Physics of Fullerenes and Related Materials*; Kamat, P. V., Guldi, D. M., Kadish, K. M., Eds.; The Electrochemical Society: Pennington, NJ, 1999; Vol. 7, and earlier volumes in this series.

(2) Martin, N.; Sachez, B.; Illescas, B.; Perez, I. *Chem. Rev.* **1998**, *98*, 2427.

(3) da Ros, D.; Prato, M. *Chem. Commun.* **1999**, 663.

(4) Prato, M.; Maggini, M. *Acc. Chem. Res.* **1998**, *31*, 519.

(5) Deviprasad, G. R.; Rahman, M. S.; D'Souza, F. *Chem. Commun.* **1999**, 849.

(6) de la Cruz, P.; de la Hoz, A.; Langa, F.; Martin, N.; Perez, M. C.; Sanchez, L. *Eur. J. Org. Chem.* **1999**, 3433.

(7) Cliffel, D. E.; Bard, A. J. *J. Phys. Chem.* **1994**, *98*, 8140.

(8) Niyazymbetov, M. E.; Evans, D. H. *J. Electrochem. Soc.* **1995**, *142*, 2655.

(9) Niyazymbetov, M. E.; Evans, D. H.; Lerke, S. A.; Cahill, P. A.; Henderson, C. C. *J. Phys. Chem.* **1994**, *98*, 13093.

(10) Fendler, J. H. In *Membrane Mimetic Chemistry*; John Wiley & Sons: New York, 1982.

(11) Chambers, C. C.; Hawkins, G. D.; Cramer, C. J.; Truhlar, D. G. *J. Phys. Chem.* **1996**, *100*, 16385.

(12) Kutner, W.; Noworyta, K.; Rahman, M. S.; Deviprasad, G. R.; D'Souza, F. In *Recent Advances in the Chemistry and Physics of Fullerenes and Related Materials*; Kamat, P. V., Guldi, D. M., Kadish, K. M., Eds.; The Electrochemical Society: Pennington, NJ, 1999; Vol. 7, p 84.

(13) Kutner, W.; Noworyta, K.; Deviprasad, G. R.; D'Souza, F. *J. Electrochem. Soc.* **2000**, *147*, in press.

(14) *SPARTAN PRO*; Wavefunction, Inc., 18401 Von Karman, Suite 370, Irvine, CA 92715.

(15) *Gaussian 98* (Revision A.7); Frisch, M. J.; Trucks, G. W.; Schlegel, H. B.; Scuseria, G. E.; Robb, M. A.; Cheeseman, J. R.; Zakrzewski, V. G.; Montgomery, J. A.; Stratmann, R. E.; Burant, J. C.; Dapprich, S.; Millam, J. M.; Daniels, A. D.; Kudin, K. N.; Strain, M. C.; Farkas, O.; Tomasi, J.; Barone, V.; Cossi, M.; Cammi, R.; Mennucci, B.; Pomelli, C.; Adamo, C.; Clifford, S.; Ochterski, J.; Petersson, G. A.; Ayala, P. Y.; Cui, Q.; Morokuma, K.; Malick, D. K.; Rabuck, A. D.; Raghavachari, K.; Foresman, J. B.; Cioslowski, J.; Ortiz, J. V.; Stefanov, B. B.; Liu, G.; Liashenko, A.; Piskorz, P.; Komaromi, I.; Gomperts, R.; Martin, R. L.; Fox, D. J.; Keith, T.; Al-Laham, M. A.; Peng, C. Y.; Nanayakkara, A.; Gonzalez, C.; Challacombe, M.; Gill, P. M. W.; Johnson, B. G.; Chen, W.; Wong, M. W.; Andres, J. L.; Head-Gordon, M.; Replogle, E. S.; Pople, J. A. Gaussian, Inc., Pittsburgh, PA, 1998.

(16) (a) Hungerbühler, H.; Guldi, D. M.; Asmus, K.-D. *J. Am. Chem. Soc.* **1993**, *115*, 3386. (b) Guldi, D. M. *J. Phys. Chem. A* **1997**, *101*, 3895.

(17) Bensasson, R. V.; Bienvenue, E.; Dellinger, M.; Leach, S.; Seta, P. *J. Phys. Chem.* **1994**, *98*, 3492.

(18) Williams, R. M.; Crielaard, W.; Hellingwerf, K. J.; Verhoeven, J. W. *Recl. Trav. Chim. Pay-Bas* **1996**, *115*, 72.

(19) Tucker, S. A.; Amszi, V. L.; Acree, W. E., Jr. *J. Chem. Ed.* **1993**, *70*, 80.

(20) Sun, Y.; Drovetskaya, T.; Bolskar, R. D.; Bau, R.; Boyd, P. D. W.; Reed, C. A. *J. Org. Chem.* **1997**, *62*, 3642.

(21) Hehre, W. J.; Shusterman, A. J.; Huang, W. W. In *A Laboratory Book of Computational Organic Chemistry*, Experiment 11; Wavefunction, Inc., 18401 Von Karman, Suite 370, Irvine, CA 92715, 1996.

(22) Cramer, C. J. In *Computational Chemistry List (CCL) Archives*, November 26, 1996.

(23) *Lange's Handbook of Chemistry*, 14th ed.; Dean, J. A., Ed.; McGraw-Hill Inc.: New York, 1992.

(24) Stewart, R. In *The Proton*: *Applications to Organic Chemistry*; Academic Press: New York, 1985.

(25) Kallies, B.; Mitzner, R. *J. Phys. Chem. B* **1997**, *101*, 2959.

(26) (a) Haddon, R. C.; Brus, L. E.; Raghavachari, K. *Chem. Phys. Lett.* **1986**, *125*, 459. (b) Haymet, A. D. *J. Chem. Phys. Lett.* **1985**, *122*, 421. (c) Hale, P. D. *J. Am. Chem. Soc.* **1986**, *108*, 6087.

(27) Suzuki, T.; Maruyama, Y.; Akasaka, T.; Ando, W.; Kobayashi, K.; Nagase, S. *J. Am. Chem. Soc.* **1994**, *116*, 1359.

(28) Ford, W. T.; Nashioka, T.; Qui, F.; D'Souza, F.; Choi, J.-p.; Kutner, W.; Noworyta, K. *J. Org. Chem.* **1999**, *64*, 6257.

(29) da Ros, T.; Prato, M.; Carano, M.; Ceroni, P.; Paulucci, F.; Roffia, F. *J. Am. Chem. Soc.* **1998**, *120*, 11645.